Jurnal Teknologi

Full paper

The Effects of Oil Supply Pressure at different Groove Position on Temperature and Pressure Profile in Journal Bearing

Mohamad Ali Ahmad[a*], Salmiah Kasolang[a], R. S. Dwyer-Joyce[b], Aidah Jumahat[a]

[a]*Faculty of Mechanical Engineering, Universiti Teknologi MARA, Malaysia*
[b]*The Leonardo Centre for Tribology, Department of Mechanical Engineering, University of Sheffield, UK*

*Corresponding author: alie_76_02@yahoo.com

Article history

Received :17 December 2013
Received in revised form :
13 January 2014
Accepted :25 January 2014

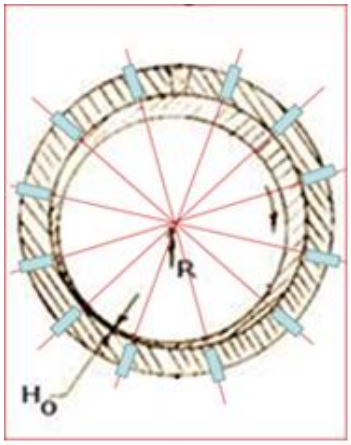

Abstract

The effects of oil supply pressure on the temperature and pressure at different groove locations on a hydrodynamic journal bearing were investigated. A journal with a diameter of 100 mm and a ½ length-to-diameter ratio was used. The supply pressure was set to 0.2, 0.5, and 0.7 MPa at seven different groove locations, namely, -45°, -30°, -15°, 0°, +15°, +30°, and +45°. Temperature and pressure profiles were measured at speed values of 300, 500, and 800 rpm with 10 kN radial load. The results show that the change in oil supply pressure simultaneously reduced the temperature and increased the pressure profile.

Keywords: Hydrodynamic lubrication; inlet pressure; journal bearing; Sommerfeld number

Abstrak

Kesan daripada tekanan masuk cecair pelincir keatas suhu dan tekanan pada kedudukan salur yang berbeza untuk gegalas jurnal hidro-dinamik telah dikaji. Jurnal berdiameter 100mm dan nisbah ½ panjang kepada diameter digunakan dalam kajian. Tekanan masuk telah ditetapkan pada tekanan 0.2, 0.5 dan 0.7 MPa di tujuh kedudukan salur masuk yang berbeza iaitu, -45°, -30°, -15°, 0°, +15°, +30°, and +45°. Profil suhu dan tekanan diukur pada kelajuan 300, 500 dan 800 putaran per minit dan daya jejarian 10 kN. Hasil kajian mendapati perubahan tekanan cecair pelincir masuk menunjukkan penurunan suhu yang mendadak dan kenaikan kepada profil tekanan.

Kata kunci: Hidrodinamik bendalir; tekanan masuk; gegalas jurnal; nombor sommerfeld

1.0 INTRODUCTION

Journal bearings are commonly found in numerous types of mechanical equipment. The main functions of journal bearings are to support radial load, facilitate motion, and transmit power. A typical journal bearing can be presented by a plain cylindrical sleeve (bushing) wrapped around a journal (shaft) [1]. Journal bearings adopt various forms depending on their application, and operate with a small clearance on the order of 1/1000 of the journal radius. This clearance is filled with a lubricant layer is responsible for the load-carrying capacity of the journal bearing. The lubrication mechanism in the journal bearing, often referred to as hydrodynamic lubrication, has been widely studied. Hydrodynamic fluid film lubrication occurs when the journal and bearing surfaces are completely separated by the established fluid layer. In the case of journal bearings, the oil film requires sufficient thickness to prevent metal-to-metal contact. The lubricant reduces friction and abrasion, prevents corrosion, and conducts heat generated by friction. Several important parameters or characteristics of hydrodynamic lubrication, such as film thickness, viscosity, pressure, temperature, and friction, are considered during the development or design stage of a journal bearing to achieve optimum operations.

Previous studies [2-5], have investigated viscosity, film thickness, temperature, and pressure in relation to journal bearings, and have conducted experiments concerning oil supply pressure and its thermal effects on journal bearings [6-8]. Recent studies [9, 10] have found that oil supply pressure and oil groove position affect the pressure profile, torque, and frictional force in journal bearings. In the present study, the effects of oil supply pressure and groove location on fluid friction and torque in hydrodynamic journal bearings are investigated.

1.1 Oil Groove Supply

In the hydrodynamic analysis, oil supply was assumed to be available to flow into the bearing at least as fast as it leaked out. Lubricant lost as a result of side leakage must be compensated for to prevent the depletion of lubricant inside the bearing. Ideally, the groove should be the same length as the bearing,

however, this similarity in length would cause all of the lubricant to leak from the sides of the groove [11].

In this experimental study, a short-angle groove type was used. The lubricant oil supplied to the bearing was pressurized. Pressurized lubricant supply can reduce lubricant heating and viscosity loss, and prevent shaft-to-bush contact during starting and stopping, modify vibration stability, and suppress cavitation. Sufficient oil supply flow can be calculated using Couette flow. Costa *et al.* [8] reported that increasing oil supply pressure can reduce operating temperature and increase maximum circumferential hydrodynamic pressure. This result is consistent with those of [6] which concluded that oil supply pressure and the geometry of the feed control determine the cooling effects.

1.2 Temperature in Journal Bearing

Temperature monitoring is an established technique for detecting overheating and preventing hydrodynamic bearing damage [12]. As reported by Moreno *et al.* [13], a significant number of numerical studies has been devoted to studying the steady-state temperature of journal bearings. In their study, the main difficulty was found to be associated with the exponential dependency of viscosity on temperature.

Mishra *et al.* [14], examined the temperature profile of an elliptic bore journal bearing and concluded that the pressure was reduced and duplicated with increasing non-circularity, specifically after a non-circularity of 0.3. The temperature rise was found to be less in the case of journal bearings with higher non-circularity values. The study assumed that the non-circularity was elliptical. Numerical solutions using the Reynolds and Energy equations were performed to outline the temperature profile. An early study on temperature distribution in journal bearings showed that load capacity is generally less than that predicted by classical isothermal theory [15].

Effective temperature is commonly used to calculate the effective viscosity in operating journal bearings. The effective temperature T_{eff} can be calculated using the following equation [1]:

where, T_{in} = input temperature,
ΔT = temperature rise of inlet to outlet

(1)

The temperature rise in degree Celsius of the lubricant from the inlet to outlet can be determined from the performance chart by Raimondi and Boyd [16]. In some cases effective temperature was approximated by measuring the outlet temperature of the bearing because the rise temperature was not known [17]. In the present study, the validity of using effective temperature is investigated given various levels oil supply pressure at different oil groove positions.

1.3 Pressure in Journal Bearing

The pressure on the journal bearing can be plotted by solving the Reynolds equation [18, 19]. This differential equation governs the pressure distribution in fluid film lubrication for incompressible fluid.

The Reynolds equation forms the foundation of fluid film lubrication theory. From this equation, parameters, such as the geometry of the surface, relative sliding velocity, the properties of the fluids, and the magnitude of the normal load can be determined.

In this study, bearing length $\boldsymbol{L}$ over bearing diameter $\boldsymbol{D}$ ratio ($\boldsymbol{L/D}$) is equal to 0.5. From this value, the Sommerfeld number was calculated using the following equations [20],

$$S = \left(\frac{r}{c}\right)^2 \frac{\mu N}{P} \quad (2)$$

where, $\boldsymbol{\mu}$ is viscosity (Pa.s),
$\boldsymbol{N}$ is speed (rps),
$\boldsymbol{r}$ is journal radius (m),
$\boldsymbol{c}$ is clearance (m) and
$\boldsymbol{P}$ is radial load per unit of projected bearing area (N/m^2).

Equation (2) was used to obtain the predicted values of eccentricity ratio, friction coefficient, maximum film pressure, position of maximum film pressure, and the position of minimum film thickness using Raimondi and Boyd charts. These predicted values are used for validation purposes with the following assumptions: smooth surface; Newtonian fluid; laminar flow and force resulting from the acceleration of the fluid and body forces are small compared with the surface force

2.0 EXPERIMENTAL PROCEDURES

The journal bearing test rig used in this study to characterize the temperature and pressure profiles is shown in Figure 1. A journal with a diameter of 100 mm and a length-to-diameter ratio of one half was used. The bearing part was modified to accommodate 12 thermocouples and 12 pressure transducers fixed around the journal bearing circumference 30-degree intervals, as shown in Figure 2. The journal was then mounted horizontally into the bearing. A pneumatic bellows was used to apply the required load. The maximum speed of the journal test rig was 1000 rpm. The speeds used for testing were 300, 500, and 800 rpm. In a two-component gel, it is easy to modify the molecular structure of either of the two components.

A single groove 40 mm in length, 10 mm in width, and 5 mm in depth was used in this study. During the tests, the journal bearing was run at load of 10 kN.

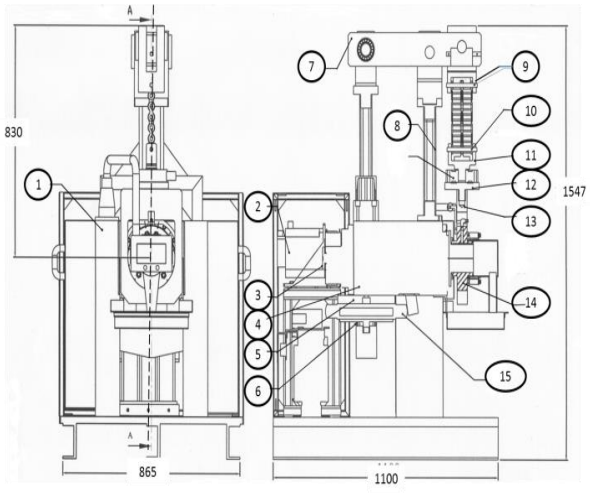

Figure 1 Diagram of Journal Bearing test rig. 1) Support structure, 2)Motor, 3)Motor bracket, 4)Spindle assy. 5)Bellow top plate, 6)Bellow guide plate, 7)Loading Lever, 8)Pivot assembly, 9)Chain, 10)Chain holder, 11)Load Cell holder, 12) Load Cell, 13)Loading plate, 14)Journal bearing and 15) Pneumatic bellows

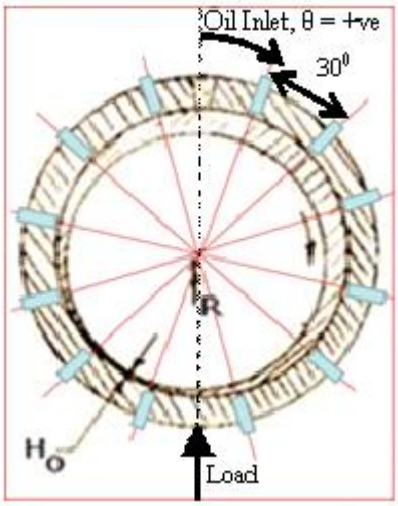

Figure 2 Temperature sensor and pressure transducer locations

The oil supply groove was positioned at -45°, -30°, -15°, 0°, 15°, 30°, and 45°.The detailed test bearing dimensions, lubricant properties, and operating parameters are given in Table 1. The lubricant temperature and pressure profiles were measured using the 12 thermocouple wires and 12 pressure transducers mounted around the bearing circumference. The pressure transducers measured fluid pressure developed through holes bored to within 0.5 mm from the bearing surface [12, 21]. Three additional thermocouples were installed to measure the room temperature as well as lubricant inlet and outlet temperatures. The oil inlet supply pressure was regulated using a power pack lubrication system and increased from 0.2 MPa to 0.7 MPa throughout the experiments. These inlet pressures were monitored using a PSAN-L1CPV model digital pressure sensor.

Table 1 Dimensions of test bearing, lubricant properties, operating parameters and sensor specification

Parameter	Values
Journal diameter, D	100 mm
Bearing length, L	50 mm
Radial clearance, c	52 µm
Load applied, W	10 and 20kN
Journal speed,	300 – 800 rpm
Lubricant type Lubricant viscosity	Shell Tellus S2 M 68 cSt @ 40^{O}C 8.8 cSt @ 100^{O}C
Pressure Sensor	
Model	MEAS (M5156)
Range	10 MPa
Accuracy	0.001 ± 1% MPa
Temperature sensor	
Model	PT 100
Range	0^{O}C – 100^{O}C
Accuracy	± 1% of measured temperature

3.0 RESULTS AND DISCUSSION

The experimental results for the temperature and pressure profiles are plotted in Figure 3 to 9. Figure 4(a) shows the corresponding temperature profiles at a speed of 300 rpm and load of 10 kN. The groove positions were set at -45°, -15°, 15°, and 45° at different oil supply pressure values (0.2, 0.5, and 0.7 MPa). Figure 4(b) shows the corresponding temperature profiles for the groove positions of -30°, 0°, and 30°.

In both figures, the temperature at the oil inlet supply position increases when oil supply pressure increases. However, the temperature profile of the journal bearing decreases as the oil pressure supply increases. In Figure 3, the oil supply location at 45^{0} at 0.7 MPa shows the lowest temperature profile. In all cases, the temperature profiles exhibit an increasing trend before the minimum film thickness, because the friction between the fluid layers is expected to increase as it enters the converging region. The temperature difference was observed to vary (by up to 5 °C) at different groove locations and oil supply pressures.

The effective temperature calculated from Raimondi and Boyd charts using Equation 1 was higher than the average temperature measured between the inlet and outlet sensors. The difference was about 5 °C.

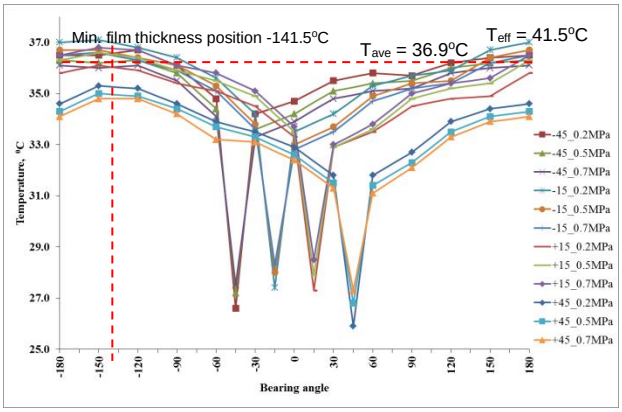

(a)

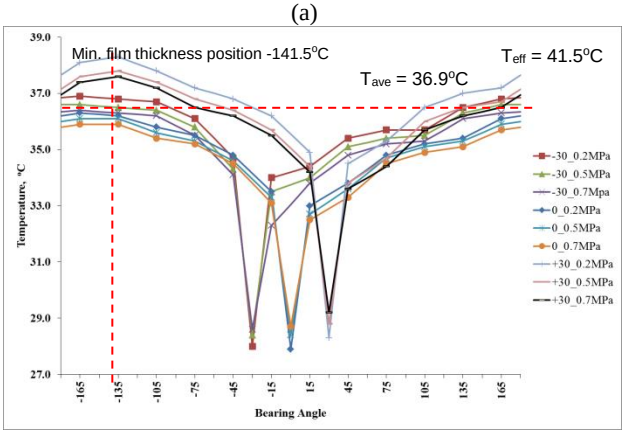

(b)

Figure 3 Temperature profiles for various oil supply pressured at 300 rpm and 10 kN. (a) Oil groove location at -45°, -15°, 15°, and 45° . (b) Oil groove location at -30°, 0°, and 30°

Figure 4 shows the temperature profiles at 500 rpm and 10 kN load. In Figure 4(a), the temperature profiles at 45° remain the lowest, as in the case of 300 rpm for the same load value. Increasing the oil supply pressure from 0.2 MPa to 0.5 MPa tends to decrease the temperature. However, at 500 rpm,

increasing oil supply pressure from 0.5 MPa to 0.7 MPa does not affect the temperature profiles.

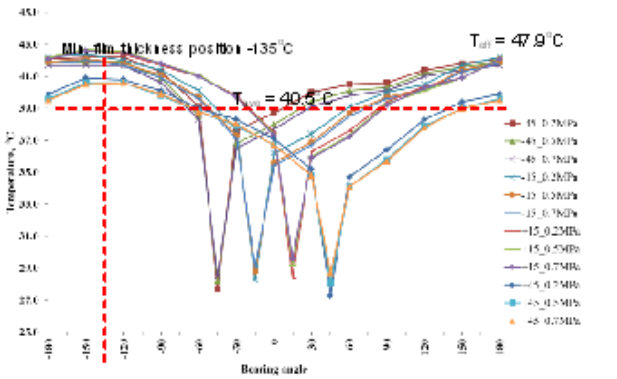

(a)

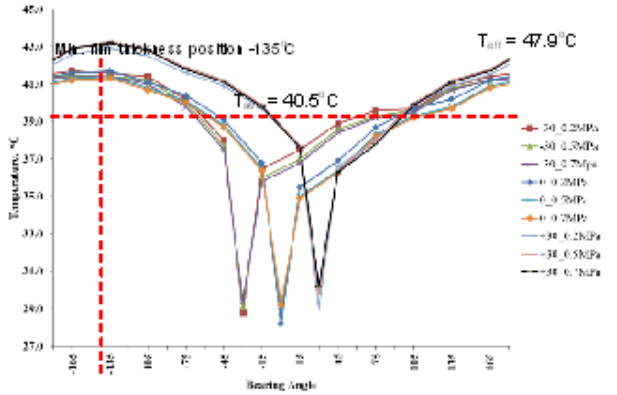

(b)

Figure 4 Temperature profiles for different oil supply pressure at 500 rpm and 10 kN. (a) oil groove location at -45°, -15°, 15°, and 45° (b) oil groove location at -30°, 0°, and 30°.

The calculated effective temperature values at 500 rpm (Figure 4(a) and 4(b)) are higher than those at 300 rpm (Figure 3). This result was expected because increasing speed tends to increase bearing number, S (Equation (2)), and hence the bearing friction.

In Figure 4(b), the temperature profiles for the oil groove locations at -30° and 0° show that oil inlet supply pressure has less effects on the temperature profiles compared to Figure 3(b), particularly in the vicinity of the minimum film thickness, as shown by the overlapping profiles.

Figure 5 is plotted for a journal speed of 800 rpm at a load of 10 kN. Both Figure 5(a) and 5(b) show that for the groove position at 45°, the temperature profile before the minimum film thickness region is relatively lower than the others. For the groove location at 15°, the oil inlet pressure supply has an effect at this speed, with a temperature difference of 2 °C.

Compared with the other groove locations and oil supply pressures, this 15° location has the highest temperature profiles. The difference between the predicted and experimental effective temperature values is about 10 °C at an oil inlet supply pressure of 0.2 MPa.

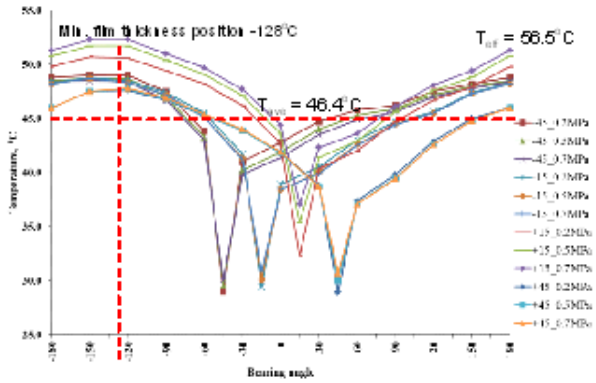

(a)

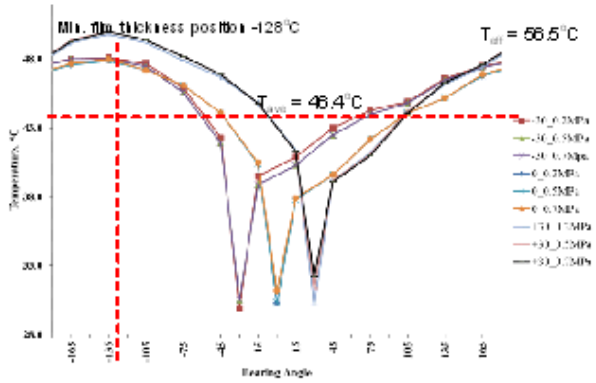

(b)

Figure 5 Temperature profiles for various oil supply pressures at 800 rpm and 10 kN. (a) Oil groove location at -45°, -15°, 15°, and 45°. (b) Oil groove location at -30°, 0°, and 30°

Based on Figure 3 to 5, the temperature profiles obtained for different oil supply pressure values at different groove positions are less affected at a higher speed (800 rpm). Nevertheless, at a lower speed (300 rpm), the temperature profiles obtained are more scattered, that is, easily differentiable.

Figure 6 shows the pressure profiles at a speed of 300 rpm and load of 10 kN at different oil groove positions and oil supply pressure values. Figure 6(a) shows the pressure profiles at the oil groove positions at -45°, -15°, 15°, and 45°. Figure 6(b) shows the pressure profiles at the oil groove positions at -30°, 0°, and 30°. The position of minimum film thickness, terminating pressure, maximum pressure, and the value of the maximum pressure obtained from the Raimondi and Boyd charts are indicated in the plot for comparison purposes

The pressure profiles in Figure 6 are plotted separately. In Figure 6(a), transducers are present at the same locations when the oil inlet supply groove changes from -30° to 0° to 30°. Similarly, in Figure 7(b), the oil supply groove positions at -45°,-15°, 15°, and 45° are grouped together for easier data analysis and comparison.

Generally, based on Figure 6, increasing oil inlet supply pressure increases the pressure profile. In Figure 6(a), the oil inlet supply pressure of 0.7 MPa at the 45° groove location exhibits the highest pressure profile, unlike what was observed earlier in the temperature profiles shown in Figure 3 to 5. In

Figure 6(b), the oil inlet supply pressure of 0.7 MPa at 0° exhibits the highest pressure profiles.

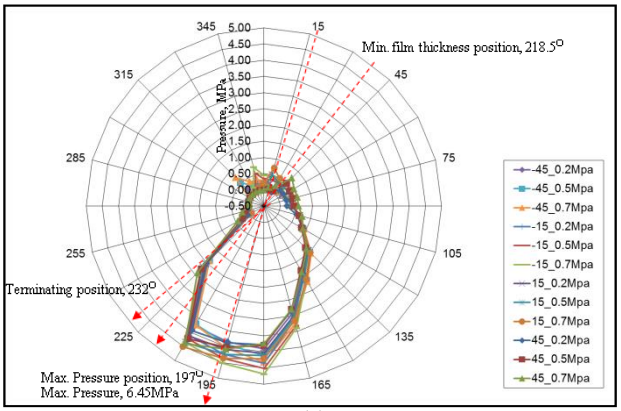

(a)

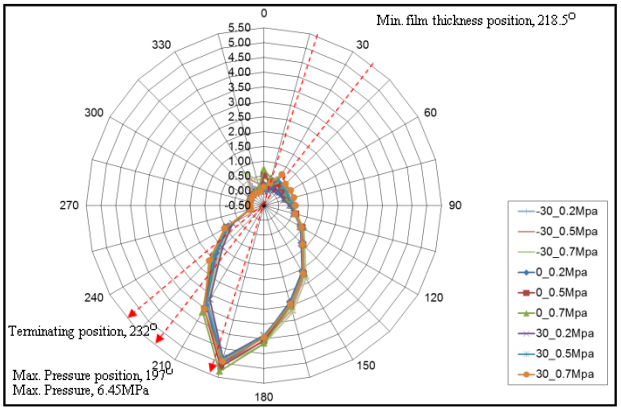

(b)

Figure 6 Pressure profiles for different oil supply pressures at 300 rpm and 10 kN. (a) Oil groove location at -45°, -15°, 15°, and 45°. (b) Oil groove location at -30°, 0°, and 30°.

Figure 7 show the pressure profiles at 300 rpm and 20 kN. The predicted values for minimum film thickness location, maximum pressure location, terminated pressure location, and maximum value obtained from the Raimondi and Boyd charts were calculated for these operating conditions. For the position of minimum film thickness, the value changes from 211.5° at 10 kN to 218.5° at 20 kN. The change in maximum pressure is from 6.45 MPa to 15.38 MPa, a 58.06% increase. Based on Figure 7, the recorded change in experimental maximum pressure is 47.6%. Although the experimental change percentage is lower, the experimental maximum pressure value is higher.

In Figure 7(a), the pressure profiles obtained before the minimum film thickness (in the region of 165° to 225°) are more differentiable. In Figure 7(b), at the same speed and loads, the pressure profiles obtained are more consistent with a distinct overlapping of profiles. The highest pressure profile was recorded at 0.7 MPa oil inlet supply pressure at the 0° oil groove location.

Figure 8 shows the pressure profiles for 500 rpm and 10 kN. With reference to Figure 6, the predicted values for film thickness position, terminating pressure position, and maximum pressure position in Figure 9 increase from 211.5° to 225°, 221° to 241°, and 194.8° to 197°, respectively. As expected, increasing the speed with other parameters remaining constant tends to cause the journal to climb higher, in turn causing the angles to increase.

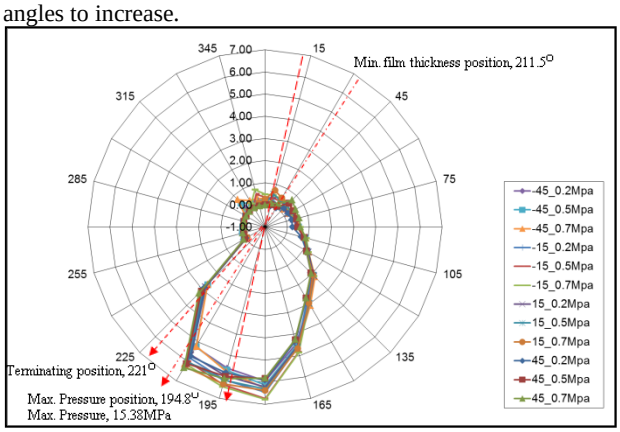

(a)

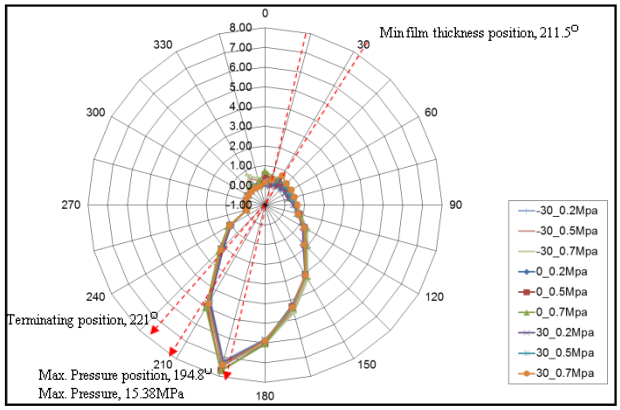

(b)

Figure 7 Pressure profiles for different oil supply pressures at 300 rpm and 20 kN. (a) Oil groove location at -45°, -15°, 15°, and 45°. (b) Oil groove location at -30°, 0°, and 30°.

Figure 8(a) shows that increasing oil pressure supply at different oil groove locations for the region of 135° to 225° affects the recorded pressure profiles. An oil supply pressure of 0.7 MPa at the 45° groove location produces the lowest value at the region of 135° to 180°, and increases until 210°. In Figure 9(b), an oil pressure supply of 0.7 MPa at the initial position of 0° produces the highest pressure profile before the minimum film thickness.

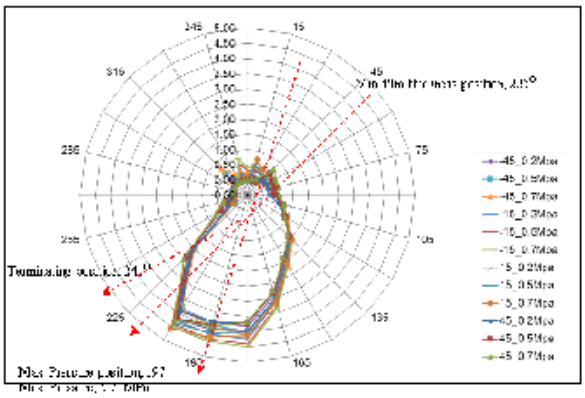

(a)

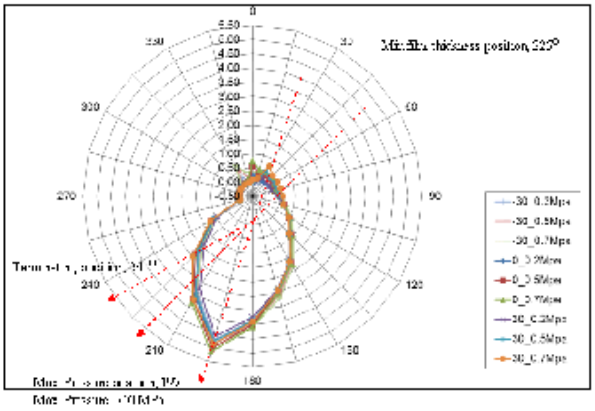

(b)

Figure 8 Pressure profiles for different oil supply pressures at 500 rpm and 10 kN. (a) Oil groove location at -45˚, -15˚, 15˚, and 45˚. (b) Oil groove location at -30˚, 0˚, and 30˚

The pressure profiles obtained at 800 rpm are plotted in Figure 9. At the same load of 10 kN, the predicted value of maximum pressure obtained at 800 rpm is higher than those at 300 and 500 rpm, with a maximum difference of 20%. The experimental maximum pressure exhibits an opposite trend, whereby the value decreases with increasing speed, with a maximum difference of 3%.

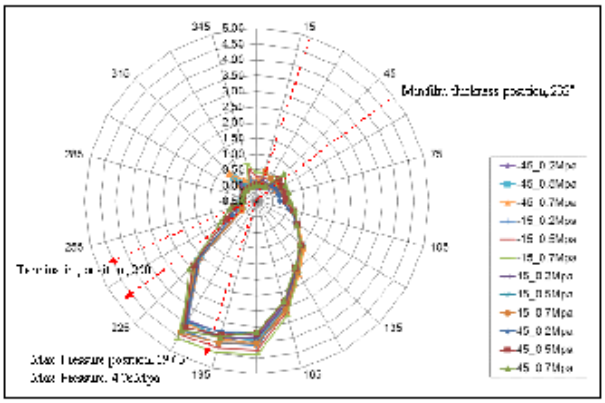

(a)

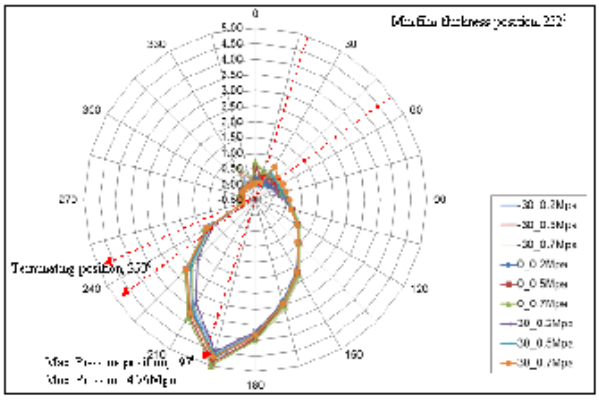

(b)

Figure 9 Pressure profiles for different oil supply pressures at 800 rpm and 10 kN. (a) Oil groove location at -45˚, -15˚, 15˚, and 45˚. (b) Oil groove location at -30˚, 0˚, and 30˚

The pressure profiles obtained at the region extending from 180˚ to 225˚ are distinct and differentiable. In Figure 9(b), the highest pressure profile recorded within this region is at 0.7 MPa at 0˚, whereas the lowest pressure profile is at 0.2 MPa at +30˚.

4.0 CONCLUSION

Experimental measurements of temperature and pressure profiles for different oil supply pressure values at different groove locations in the hydrodynamic lubrication journal bearing were carried out. The experimental results on the effects of different oil inlet supply pressure values at different groove locations for different speed and load ranges were presented. From the specific experimental operating conditions, the following conclusions were drawn:

i. The temperature at the inlet point increases when oil supply pressure increases. The temperature profile of the journal bearing tends to decrease when oil supply pressure increases. The nearer the oil supply groove, to the minimum film thickness position in the converging section, the lower the temperature profiles obtained. In the experiment, changing the groove location from 0˚ to +45˚ significantly reduced the temperature profiles. Increasing oil inlet supply pressure from 0.2 to 0.7 MPa tends to further reduce the temperature profiles.

ii. Increasing oil supply pressure at different oil groove locations tends to affect the pressure profiles of the journal bearing lubrication. In this study, increasing the oil inlet supply pressure increased the lubricant pressure profiles in the journal bearing. Changing the oil groove locations from the initial position tended to reduce the pressure profiles. The maximum pressure value obtained at 30˚ was slightly lower than the pressure value obtained at 0˚, that is, the initial position.

Acknowledgement

The authors would like to thank the Ministry of Higher Education of Malaysia (MOHE) for the financial support extended to this study through the MyBrain, E-science, FRGS, and ERGS Grant awards. The authors are also indebted to the

Research Management Institute of UiTM for facilitating this project.

References

[1] B. J. Hamrock, S. R. Schmid, and B. O. Jacobson. 2004. *Fundamentals of fluid film lubrication*, 2nd ed. New York: Marcel Dekker.

[2] S. Kasolang, M. A. Ahmad, and R. S. D. Joyce. 2010. "Viscosity profile measurement in journal bearing by shear ultrasonic reflection," in *Computer Engineering and Technology (ICCET), 2010 2nd International Conference on*, pp. V5-41-V5-45.

[3] S. Kasolang, M. A. Ahmad, and R. S. Dwyer Joyce. 2011. "Measurement of circumferential viscosity profile in stationary journal bearing by shear ultrasonic reflection," *Tribology International*, vol. 44, pp. 1264-1270.

[4] S. Kasolang, M. A. Ahmad, R. Dwyer-Joyce, A. Jaffar, M. A. A. Bakar, N. H. Saad, and A. Jumahat. 2012. "Experimental Study of Temperature profile in a Journal Bearing.pdf," in *1st Joint Symposium on System-Integrated Intelligence: New Challenges for Product and Production Engineering*, Hannover, Germany, pp. 43-45.

[5] S. Kasolang, M. A. Ahmad, R.-D. Joyce, and C. F. M. Taib. 2012. "Preliminary Study of Pressure Profile in Hydrodynamic Lubrication Journal Bearing," *Procedia Engineering*, vol. 41, pp. 1743-1749.

[6] H. So and J. A. Shieh. 1987. "The cooling effects of supply oil on journal bearings for varying inlet conditions," *Tribology International*, vol. 20, pp. 79-89.

[7] B. C. Majumdar and A. K. Saha. 1974. "Temperature Distribution in Oil Journal Bearing," *Wear*, vol. 28, p. 8.

[8] L. Costa, M. Fillon, A. S. Miranda, and J. C. P. Claro. 2000. "An Experimental Investigation of the Effects of Groove Location and Supply Pressure on the THD Performance of a Steadily Loaded Journal Bearing," *Journal of Tribology*, vol. 122, p. 6.

[9] M. A. Ahmad, S. Kasolang, R. S. Dwyer Joyce, and N. R. Abdullah. 2013. "The Effects of Oil Supply Pressure on the Circumferential Pressure Profile in Hydrodynamic Journal Bearing," *Applied Mechanics and Materials*, vol. 315, p. 6.

[10] M. A. Ahmad, S. Kasolang, and R. S. Dwyer Joyce. 2013. "Experimental Study of Oil Supply Pressure Effects on Bearing Friction in Hydrodynamic Lubrication," *Applied Mechanics and Materials*, vol. 315, p. 5.

[11] G. W. Stachowiak and A. W. Batchelor. 2005. *Engineering tribology*, 3rd ed. Amsterdam ; Boston: Elsevier Butterworth-Heinemann.

[12] S. B. Glavatskih. 2004. "A method of temperature monitoring in fluid film bearings," *Tribology International*, vol. 37, pp. 143-148.

[13] J. A. Moreno Nicolás, F. C. Gómez de León Hijes, and F. Alhama. 2007. "Solution of temperature fields in hydrodynamics bearings by the numerical network method," *Tribology International*, vol. 40, pp. 139-145.

[14] P. C. Mishra, R. K. Pandey, and K. Athre. 2007. "Temperature profile of an elliptic bore journal bearing," *Tribology International*, vol. 40, pp. 453-458.

[15] B. C. Majumdar and A. K. Saha. 1974. "Temperature Distribution in Oil Journal Bearings," *Wear*, vol. 28, pp. 259 - 266.

[16] J. Shigley and C. Mischke. 1983. "Lubrication and Journal Bearings," *Mechanical Engineering Design, New York, McGraw-Hill*, p. 562.

[17] S. Kasolang. 2008. "An ultrasonic investigation of various aspects of hydrodynamic lubrication in a journal bearing," Degree of Doctor of Philosophy, Department of Mechanical Engineering, University of Sheffield.

[18] D. Dowson. 1962. "A Generalised Reynolds Equations for Fluid-Film Lubrication," *Int. J. Mech. Sci.*, vol. 4, p. 12.

[19] B. Bhushan. 2002. *Introduction to tribology*. New York: John Wiley & Sons.

[20] R. C. Juvinall and K. M. Marshek. 2006. *Fundamentals of machine component design*, 4th ed. Hoboken, NJ: John Wiley & Sons.

[21] T. Syverud. 2001. "Experimental investigation of the temperature fade in the cavitation zone of full journal bearings," *Tribology International*, vol. 34, pp. 859-870.